Society For Biomaterials

Interplay between long- and short-range interactions drives neuritogenesis on stiff surfaces

Guillaume Lamour,[1]* Sylvie Souès,[2] Ahmed Hamraoui[1,3]

[1]Université Paris Descartes, UFR Biomédicale, 45 rue des Saints-Pères, 75006 Paris, France
[2]Université Paris Descartes, Régulation de la Transcription et Maladies Génétiques, FRE3235, 45 rue des Saints-Pères, 75006 Paris, France
[3]CEA Saclay, Service de Physique et Chimie des Surfaces et Interfaces, 91191 Gif-sur-Yvette, France

Received 24 March 2011; revised 24 June 2011; accepted 17 July 2011
Published online 27 September 2011 in Wiley Online Library (wileyonlinelibrary.com). DOI: 10.1002/jbm.a.33213

Abstract: Substrate factors such as surface energy distribution can affect cell functions, such as neuronal differentiation of PC12 cells. However, the surface effects that trigger such cell responses need to be clarified and analyzed. Here we show that the total surface tension is not a critical parameter. Self-assembled monolayers of alkylsiloxanes on glass were used as culture substrates. By changing the nanoscale structure and ordering of the monolayer, we designed surfaces with a range of dispersive (γ^d) and nondispersive (γ^{nd}) potentials, but with a similar value for total free-energy ($50 \leq \gamma^d + \gamma^{nd} \leq 55$ m*N* m^{-1}). When seeded on surfaces displaying $\gamma^d/\gamma^{nd} \leq 3.7$, PC12 cells underwent low level of neuritogenesis. On surfaces exhibiting $\gamma^d/\gamma^{nd} \geq 5.4$, neurite outgrowth was greatly enhanced and apparent by only 24 h of culture in absence of nerve growth-factor treatment. These data indicate how the spatial distribution of surface potentials may control neuritogenesis, thus providing a new criterion to address nerve regeneration issues on rigid biocompatible surfaces. © 2011 Wiley Periodicals, Inc. J Biomed Mater Res Part A: 99A: 598–606, 2011.

Key Words: PC12 cells, neurite outgrowth, self-assembled monolayers (SAMs), surface energy, aminosilane

How to cite this article: Lamour G, Souès S, Hamraoui A. 2011. Interplay between long- and short-range interactions drives neuritogenesis on stiff surfaces. J Biomed Mater Res Part A 2011:99A:598–606.

INTRODUCTION

Neuronal differentiation is critical to nervous tissue regeneration after injury, and a critical step in this process is proper adhesion on a substrate.[1–3] The initiation of a neurite relies on extracellular signals, such as spatial, chemical, and mechanical inputs, which act together with the genetic program to regulate cell functions.[4] Several studies demonstrate the ability of cells, especially nerve cells, to sense substrate nanoscale topography,[5–7] surface chemistry,[8–10] and substrate compliance.[11–13] Substrates with spatially varied surface adhesiveness can orientate the growth of preexisting neurites along the direction of the gradients,[14] and heterogeneous distribution of nonspecific cell–substrate interactions can even trigger neuritogenesis.[15] Markedly, nanoscale chemical heterogeneities were recently proven to impact both cell adhesion and ability to differentiate into neuronal cells.[16] However, the exact role of the surface tension and its spatial variation is still unclear and further experiments should clarify the surface adhesion parameters that drive neuritogenesis.

Clonal line PC12 pheochromocytoma cells express the transmembrane TrkA and p75 receptors to nerve growth factor (NGF),[17,18] and differentiate into a neuronal phenotype when challenged by appropriate NGF concentrations.[19] Hence PC12 cells constitute a relevant model to study neuronal differentiation mechanisms. Substrate factors can associate with NGF[20] or even substitute to NGF[21,22] in stimulating differentiation of PC12 cells, and several key inducers of PC12 neuronal differentiation in NGF-free medium have been identified on soft substrates composed of extracellular matrix (ECM) proteins such as collagen, fibronectin, and laminin,[21] or of ECM derived from astrocytes.[22]

In our two previous studies,[15,16] we showed that PC12 differentiation in NGF-free medium is achievable also when cells are seeded on stiff substrates. Glass surfaces coated with self-assembled monolayers (SAMs) of alkylsiloxanes displayed local gradients in surface free-energy, which promoted neurite extension and expression of neuronal markers.[15] It turned out that PC12 differentiation was the

Additional Supporting Information may be found in the online version of this article.
**Present address of Guillaume Lamour:* University of British Colombia, Centre for High-Throughput Biology, 183F-2125 East Mall, Vancouver, British Colombia V6T 1Z4, Canada.
Correspondence to: G. Lamour; e-mail: lamour@chibi.ubc.ca
Contract grant sponsors: French Ministry of Research; The University of Paris Diderot; The IFR95; The University of Paris Descartes

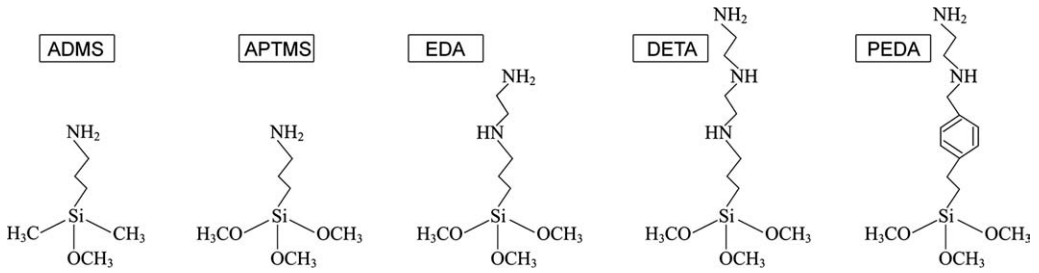

FIGURE 1. Schematics of NH_2-terminated molecules used to modify glass surfaces. Molecules were grafted onto clean glass surfaces by chemisorption from the liquid phase. APTMS, EDA, DETA, and PEDA do cross-link during SAMs formation, contrary to ADMS, that can only bind glass surfaces through one covalent bond, following hydrolysis of its unique OCH_3 leaving group.

consequence of surface effects induced by nanoscale gradients in wettability.[16] More precisely, these experiments showed that a nanoscale mixture of CH_3 and OH groups triggered both PC12 adhesion and neuritogenesis, while well-ordered homogeneous substrates made of either OH or CH_3 groups, did not favor PC12 adhesion. Cells responded favorably to spatial variations of London-dispersion interaction (long-range, γ^d; $<$100 nm) and nondispersive (short-range, γ^{nd}; $\sim$3 Å) components in substrate surface tension. However, we did not determine whether the total surface free-energy ($\gamma_s = \gamma^d + \gamma^{nd}$) had a critical impact, as levels of neuritogenesis were increased together with short-range interactions that cells experienced (the γ^d being similar for all substrates).[16] Therefore, it has to be determined how cells react to alternative distributions of surface potentials, by designing surfaces which γ_s values are close to each other.

To alter the respective intensities of γ^d and of γ^{nd}, we used different NH_2-terminated alkylsilanes (Fig. 1). Because of the higher reactivity of NH_2 compared to (almost) apolar CH_3 groups, the control over adsorption process is rather difficult. We thus chose to modify glass surfaces from the liquid phase using the same solvent solution for all molecules. Consequently, only the differences due to the nature of the molecules (alkyl chain length, number of amine groups) can be held as responsible for distinct properties related to surface ordering, and thus to specific distributions of γ^d and γ^{nd}.

We analyzed our substrates applying the well-known Zisman plot method[23] to determine their critical surface energies (γ_c), and the Owens–Wendt theoretical model[24] to determine their surface potential components (γ^d and γ^{nd}). γ_c is an empirical value below which any liquid having a surface tension lower than γ_c will undergo complete spreading, thus theoretically forming a molecular monolayer. γ^d corresponds to instantaneous-dipole induced-dipole forces that act between atoms and molecules, and can be assimilated to Van der Waals forces in the context of this study. γ^{nd} is the term regrouping all nondispersive interactions (ionic-like electrostatic, acid–base—Lewis or Brönsted—in general, and hydrogen bonds in particular).

It is important to remark that neither absolute values of γ_c, nor the relative values of γ^d versus γ^{nd} (or absolute values of γ^d/γ^{nd}) should be considered, only by themselves, as critical triggers of specific cell responses such as neuritogenesis. Rather, they macroscopically reflect diverse nanostructures (sketched in Fig. 2) of overly simple model surfaces substantially composed of terminal amines and hydroxyl groups only. Therefore, the specific values indicated in this study for γ_c and γ^d/γ^{nd} are used to provide a convenient tool to compare our surfaces between each other, but may not apply when comparing systems which chemical nature are essentially different (for instance, polymers such as polystyrene, polycarbonate, or polysulfone, that all have different terminal groups). It is also to be noted that in this work, we assimilate the discrete spatial distribution of the energy of adhesion to local gradients in the energy of adhesion.

Our results clearly show how diverse nanoscale structures influence PC12 cell neuritogenesis and provide an insight into a formerly unknown type of cell–substrate interactions. It clearly strengthen the idea that nanoscale chemical heterogeneities, by generating surface-energy gradients, are involved as a master parameter, stronger than the surface roughness, in neurite initiation on stiff model surfaces.

MATERIALS AND METHODS

Chemicals

Chemicals were obtained from Acros Organics (Geel, Belgium), Sigma–Aldrich (St. Quentin Fallavier, France), ABCR (Karlsruhe, Germany), Fisher Scientific (Illkirch, France) and Carlo Erba Reagents (Val de Reuil, France). The sources and purity of the chemicals used are recapitulated in Table I.

Substrates preparation

Prior to use, glass coverslips (Menzel-Glaser, Braunschweig, Germany) were cleaned by immersion for 20 min in ultrasonic bath of chloroform prior to immersion in piranha solution [3:1 (v/v) concentrated sulphuric acid:40% hydrogen peroxide (Caution! Piranha solution is a very strong oxidant and is extremely dangerous to work with; gloves, goggles, and a face shield should be worn)], then thoroughly rinsed with ultrapure water and dried under a nitrogen stream. Modified coverslips eda, peda, deta, aptms, adms, respectively, were obtained by immersion of the clean glass in a solution of 2% EDA, PEDA, DETA, APTMS, ADMS, respectively, and of 94% methanol, 4% H_2O, 1 m*M* acetic acid. The

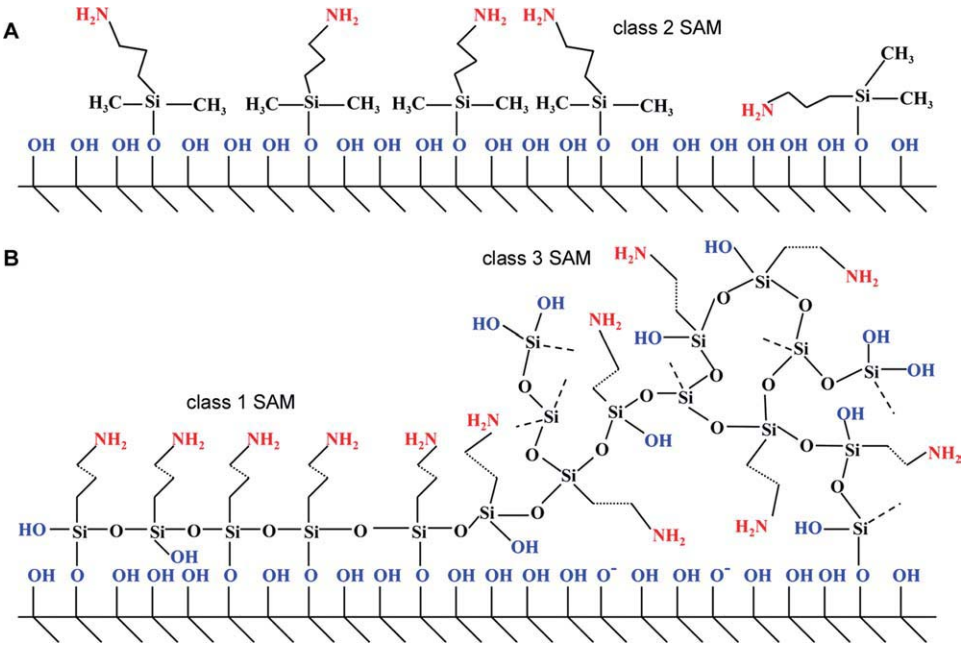

FIGURE 2. Sketches representing potential nanostructures of NH_2-terminated self-assembled monolayers (SAMs) used as substrates for PC12 cell culture. Class 1 SAMs are well-ordered with all-trans conformation of alkyl chains, class 2 SAMs are disordered but limited to monolayer formation, and class 3 SAMs are highly disordered, with possible multilayer formation and higher chemical heterogeneity. (A) ADMS, being a *mono*methoxysilane, forms a class 2 SAM. (B) APTMS, EDA, DETA, and PEDA, being *tri*methoxysilanes, form surfaces that are most probably the result of a combination between well-ordered (i.e., class 1) and highly disordered (i.e., class 3) organizations. One goal of this study is to determine what organization predominates for each molecules, according to their lateral chain length and to the number of amine groups contained by each chains (see Fig. 1). [Color figure can be viewed in the online issue, which is available at wileyonlinelibrary.com.]

relatively high amount of water, together with acetic acid, guaranteed that the hydrolysis of methoxy groups was predominant over other potential reactions[25,26] involving terminal amine groups and OH groups from the glass surface. The time of immersion always exceeded 36 h, to obtain an optimal coverage of the glass surfaces with aminosilanes, such that contact angles could not be increased. All substrates were then rinsed with methanol and either allowed to dry under a laminar flow hood, prior to cell culture, or dried under a nitrogen stream, prior to surface characterization by AFM and contact angle measurements. All treatments were carried out at room temperature and in ambient atmosphere (relative humidity $\approx$ 50%).

Potential nanostructures generated by NH_2-terminated silanized surfaces

Molecules (noted in capital letters) of various chain length and chemical nature (Fig. 1) were chosen to generate distinct surfaces (noted in minuscule letters), according to their mechanism of adsorption and to the monolayer formed on glass. According to our previous studies,[16] the resulting culture substrates can be ranked into three

TABLE I. Chemicals Used for Surface Modification and Contact Angle Measurements

Chemical	Manufacturer	Purity (%)
Ultrapure water (Elga UHQ PS MK3)	Veolia Water Systems	(ρ = 18.2 MΩ cm^{-1})[a]
Methanol	Carlo Erba Reagents	>99.9 (HPLC)[b]
Acetic acid	Carlo Erba Reagents	99.9 (RPE)
Sulphuric acid	Sigma–Aldrich	95–97
Hydrogen peroxide	Sigma–Aldrich	40 (m/v in H_2O)
Chloroform	Carlo Erba Reagents	>99.8 (ACS)
n-[3-Trimethoxysilyl)propyl]ethylendiamine (EDA)	Acros Organics	97
(3-(Trimethoxysilyl)propyl)diethylenetriamine (DETA)	Sigma–Aldrich	$\geq$85
3-Aminopropyltrimethoxysilane (APTMS)	Acros Organics	95
3-Aminopropyldimethylmethoxysilane (ADMS)	Acros Organics	97
(Aminoethylaminomethyl)phenyltrimethoxysilane (PEDA)	ABCR	90
Formamide (FA)	Fisher Scientific	$\geq$99.5
Diiodomethane (DIM)	Acros Organics	$\geq$99
α-Bromonaphthalene (αBrN)	Fisher Scientific	>96 (extra pure, SLR)

[a] Concentration in TOC (total organic carbon) is < 10 ppb.
[b] Water content is <0.01%.

TABLE II. Data Collected From Contact Angle Measurements and AFM

		adms	aptms	deta	eda	peda
θ_{H2O}	deg	57	54	62	68	70
θ_{FA}	deg	45	41	51	47	48
θ_{DIM}	deg	42	39	36	32	27
$\theta_{\alpha BrN}$	deg	34	32	25	21	18
γ_c	m*N* m^{-1}	26.4 ± 1.4	28.0 ± 1.6	37.6 ± 2.3	42.1 ± 1.1	43.6 ± 2.2
γ_s	m*N* m^{-1}	52.4 ± 1.6	54.7 ± 1.6	50.5 ± 1.5	50.2 ± 1.2	50.2 ± 1.0
γ^d	m*N* m^{-1}	37.0 ± 0.8	38.0 ± 0.8	39.8 ± 0.6	42.4 ± 0.2	43.6 ± 0.2
γ^{nd}	m*N* m^{-1}	15.4 ± 1.6	16.7 ± 1.6	10.7 ± 1.3	7.8 ± 1.0	6.6 ± 1.0
γ^d/γ^{nd}		2.4	2.3	3.7	5.4	6.6
rms (1 μm^2)	nm	0.3	0.3	0.3	0.3	0.3
rms (4 μm^2)	nm	0.4	1.4	0.4	0.3	0.4
θ_{AR}	deg	15	54	32	42	40

Contact angles (θ) were measured using water, formamide (FA), diiodomethane (DIM), and α-bromonaphthalene (αBrN), as test liquids. Uncertainty on a measured contact angle was statistically estimated to be less than 2°,[27] and taken into account in the calculations of surface energies. θ_{AR} is the difference between advancing and receding contact angles of water. The critical surface tension (γ_c) was determined from Zisman plots using contact angles of each test liquids (Fig. 3). The dispersive (γ^d) and nondispersive (γ^{nd}) values of the total surface free-energy (γ_s) were calculated from the water and αBrN fitted contact angles (see Table SII in Supporting Information). Values of the root mean square (rms) roughness (±0.1 nm) are the mean of three independent measurements.

different classes (Fig. 2) with regard to nanoscale surface organization and hence to distribution of surface energy. Being a *mono*methoxysilane, ADMS should generate a class 2 surface, which is rather homogeneous, due to monolayer formation processes that forbid multilayer formation. APTMS, EDA, DETA, and PEDA are *tri*methoxysilanes, and as such, are capable of undergoing chaotic polymerization previously to the adsorption on glass. Here, the adsorption of trimethoxysilanes can give rise either to a well-ordered (class 1) or to a disordered (class 3) organization, or to a combination of these organizations, as sketched in Figure 2. Therefore, it has to be determined what organization, ordered or disordered, will be favored for each glass-bound oligomers made of trimethoxysilanes.

Surface characterization and determination of surface energies

Details on methods in this section can be found in Ref. 16. Briefly contact angles (θ) were measured as described in a previous work.[27] The critical surface tension γ_c was calculated using the Fox–Zisman approximation[23] after measuring the contact angles of all test liquids, namely H_2O, FA, αBrN, and DIM. The Owens–Wendt theoretical model[24] was used to calculate the long-range dispersion (Lifshitz–Van der Waals; γ^d; <100 nm) and the short-range non-dispersive (electron donor/acceptor; γ^{nd}; ~3 Å) components of the surface free-energy (SFE) using contact angles of H_2O and αBrN for each solid substrate (see Table SI and Figs. S1 and S2 in the Supporting Information). It is noted that the contact angle values used for these calculations were extracted from the Zisman plots fitted data (see Table SII in the Supporting Information). Uncertainties on all surface energies were calculated considering an error of ±2° on a contact angle measurement.[27] θ_{AR}, that is the difference between the advancing and receding contact angles of water, was measured for every substrate. For roughness analyzes, we used a Bioscope™ AFM (Veeco) in air tapping mode and evaluated the root-mean-square (rms) roughness of the surfaces for areas of 1 and of 4 μm^2. For a clean glass (i.e., SAM-free) substrate, we obtained rms ≈ 0.3 nm.

PC12 cell culture

Unless otherwise specified, biological products were purchased from Invitrogen (Fisher Bioblock Scientific, Illkirch, France). PC12 cells (ATCC, CRL 1721) were maintained in Dulbecco's Modified Eagle Medium containing horse serum (5%), fetal calf serum (5%, HyClone), nonessential amino acids (1%), and antibiotics (1%). In the experiments, PC12 cells (passage numbers 7–17) were seeded onto modified glass coverslips, that had been sterilized by immersion in a solution of 70% methanol and 30% H_2O for 15 min. Cells were seeded in a small volume of the culture medium (V = 335 μL), to trap PC12 cells on the top of the modified substrates. The cell density at the time of seeding was ~10^4 cm^{-2}. Cell behavior was analyzed 24 h after seeding. No further addition of culture medium was made and, in particular, no NGF was added to the culture medium. The propensity of PC12 cells to initiate neurites was evaluated on each substrate, as described in our previous work.[16] Statistical analysis was done using the independent two-sample t test assuming an equal variance for each sample group of the same sizes (N = 3 independent measurements). p values were used to indicate levels of statistical significance.

RESULTS AND DISCUSSION

Classification of substrates in distinct surface classes

Molecules are written in capital letters (e.g., EDA) and corresponding surfaces generated from them are written in small letters (e.g., eda). Data obtained for static contact angles (θ_{AR}: advancing minus receding), γ_c, SFE potentials, and roughness analysis, are recapitulated in Table II. Two groups of surfaces arise from the values determined for γ_c (Fig. 3). In the first group, we find adms and aptms surfaces, which γ_c are quite weak (26 and 28 m*N* m^{-1}, respectively). The second group is composed of eda and peda surfaces, which γ_c are higher (42 and 44 m*N* m^{-1},

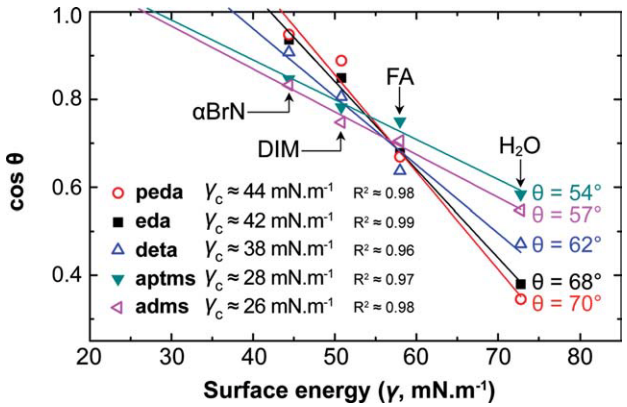

FIGURE 3. Zisman plots used to determine the critical surface tension (γ_c) of solid substrates. Contact angles (θ) were measured using water, formamide (FA), diiodomethane (DIM), and α-Bromonaphthalene (αBrN), as test liquids. γ_c values were read where the line fits intersect cos $\theta = 1$ (uncertainties on γ_c values never exceeded ± 2.3 mN m^{-1}, see Table II). γ_c indicates the propensity of each substrate to exhibit OH groups at its surface: the more OH groups are accessible to the test liquid, the higher the γ_c is. An interpretation of the results versus theoretical expectations is provided in Note S1 in the Supporting Information. [Color figure can be viewed in the online issue, which is available at wileyonlinelibrary.com.]

respectively). The γ_c of deta substrate has an intermediate value (38 mN m^{-1}).

The wettability of aptms appears to be close to that of adms, which is used here as a reference for class 2 surfaces. We hypothesize that it results from a high similarity between ADMS and APTMS molecules (see Fig. 1), and in spite of the fact that the adms surface should exhibit CH_3 groups (Fig. 2). However, it is likely that these CH_3 groups are essentially buried inside the monolayer formed on glass by ADMS molecules. In this case, adms and aptms substrates could display similar surface nanostructures (see also Note S1 in the Supporting Information). Their γ_c values indicate that, of all the substrates, adms and aptms exhibit the lowest proportion of OH groups. Indeed, the more OH groups the substrate exposes, the higher the γ_c of the substrate is, and closer to that of clean glass ($\geq$150 mN m^{-1}).[28,29] Because the adms surface is believed to be rather homogeneous, it suggests that APTMS molecules, though able to form a class 3 SAM, shape a nanostructure in which the ordered organization of monomers is favored over the disordered organization. Both adms and aptms surfaces are then to be considered as class 2 SAMs, that are homogeneous at the micrometer scale, although at the nanometer scale, surface-energy gradients can reach high values ($25 \leq \gamma_c \leq 150$ mN m^{-1}) because of the few OH groups that are scattered in a larger number of NH_2 groups. The low θ_{AR} (15°) measured for adms conforms with this hypothesis, as we found a similar value (14°) for class 2 CH_3-terminated SAMs.[16] The high θ_{AR} (54°) measured for aptms is not significative of an enhanced chemical heterogeneity compared to adms, as its surface exhibits a high nanoroughness (rms = 1.4 nm vs. 0.3 nm for all other substrates). θ_{AR} values are indeed known to increase with both chemical heterogeneity and physical roughness.[30] This nanoroughness, observed for surface areas higher than 1 μm^2 (Fig. 4), is believed to be due to the over covering of the aptms substrate by additional APTMS molecules, presumably physisorbed on it. Finally, the fact that the γ_c of aptms (28 mN m^{-1}) is a little higher than that of adms (26 mN m^{-1}) confirms that, despite being analogous to the adms substrate, aptms is the result of monolayer formation where "vertical polymerization"[31] is nonzero. Therefore, we introduce the class 2′ SAM, that is, a trimethoxysilane-based SAM which shares the properties of class 2 rather than class 3 SAMs.

High γ_c values calculated for eda (42 mN m^{-1}) and peda (44 mN m^{-1}) tend to show that their surface-exposed OH groups are in far higher proportion than in adms and aptms substrates (see also Note S2 in the Supporting Information). This illustrates the highly disordered structures displayed by both eda and peda, likely resulting of substantial vertical polymerization before and during chemical adsorption to glass. As a result, both eda and peda substrates can be considered as canonical class 3 SAMs.

It is impossible to classify the deta surface versus the other substrates considering its γ_c value only. Indeed, deta's γ_c (38 mN m^{-1}) is significantly lower than the γ_c of both eda and peda, indicating that it exposes a lower proportion of OH groups. This would correspond to a lower rate of vertical (vs. horizontal) polymerization during monolayer formation. Consequently, the ordered organization (i.e., class 1 SAM) might predominate over the disordered organization (i.e., class 3 SAM), though the γ_c of deta still remains much higher than the γ_c of both adms (26 mN m^{-1}) and aptms (28 mN m^{-1}), assigned to class 2 (or 2′) SAMs. θ_{AR} of deta (32°) strengthen this interpretation, because it reveals a chemically heterogeneous surface as opposed to the adms surface (which $\theta_{AR} = 15°$), though not as heterogeneous as eda ($\theta_{AR} = 42°$) and peda ($\theta_{AR} = 40°$), the roughness being very low for all these three substrates (rms = 0.3 nm).

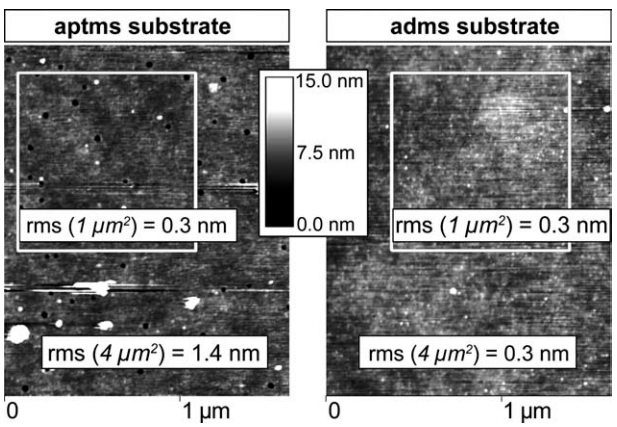

FIGURE 4. AFM images representative of the surfaces used as cell culture substrates. Roughness increase is evident for surfaces higher than 1 μm^2 (here: measured on 4 μm^2) and only for the aptms surface. For each of the other manufactured substrates, images of the surface are similar to the image of the adms surface shown here, and rms value does not increase with the area considered (rms = 0.3 nm; see also Table II).

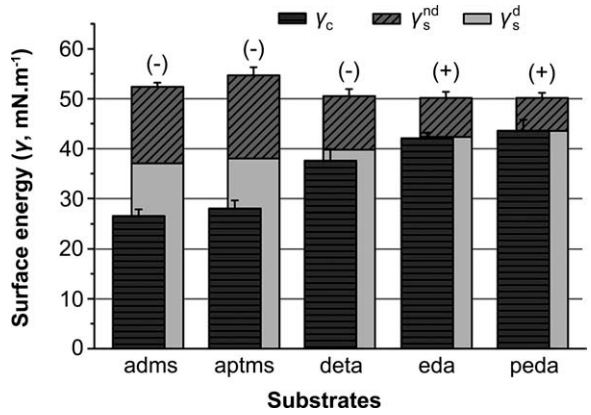

FIGURE 5. SFE components γ^d and γ^{nd} of solid substrates. γ^d and γ^{nd} were calculated through the measurements of water and αBrN contact angles, using the Owens–Wendt theoretical model. Although the distribution of γ^d and γ^{nd} vary from one substrate to another, total SFE (i.e., $\gamma_s = \gamma^d + \gamma^{nd}$) values are very similar for all substrates. PC12 cell fate, 24 h after seeding, is indicated for each of these substrates: either the cells adhered and initiate few neurites (−), or the adhesion was enhanced and the cells generated many neurites (+). Uncertainty bars relate to γ_c and γ_s values (see Table II). The Owens–Wendt model using other combinations of test liquids is discussed along with Figure S2 in the Supporting Information.

Substrates surface potentials: long-range, short-range, and total free-energy

The total SFE (i.e., $\gamma_s = \gamma^d + \gamma^{nd}$) of all substrates verify: $50.2 \leq \gamma_s \leq 54.7$ mN m^{-1} (Fig. 5). These values are of the same order of magnitude than those determined for CH_3-terminated SAMs, for which we obtained: $21.6 \leq \gamma_s \leq 59.9$ mN m^{-1}.[16] Hence it is relevant to compare CH_3- with NH_2-terminated SAMs, especially those that belong to the same surface class but differ chemically. Moreover, because here γ_s values are similar between each other, it becomes possible to determine whether γ_s is critical to PC12 cell neuritogenesis.

Each substrate verify the relation $\gamma^d > \gamma^{nd}$ (Fig. 5). Yet, the distributions of γ^d and γ^{nd} significantly differ between class 2 or 2′ surfaces (adms or aptms), where $\gamma^d/\gamma^{nd} \leq 2.4$, and class 3 surfaces (eda and peda), where $\gamma^d/\gamma^{nd} \geq 5.4$ (see Note S2 in the Supporting Information where SFE values are further discussed). As with Zisman plots, the deta surface is in between these class 2 and class 3 surfaces, displaying $\gamma^d/\gamma^{nd} = 3.7$. Therefore it is not possible to classify it considering this parameter only. However, it constitutes an alternative to the other substrates considered here, and thus makes an interesting case for cell culture experiments. The particular propensities of each substrate to stimulate neuritogenesis of PC12 cells according to surface energy parameters are discussed here after.

Differential behavior of PC12 cells according to the surface organization

The observation of PC12 cells (Fig. 6) seeded on eda, peda, adms, and aptms, previously characterized, clearly show that the total surface tension γ_s is not a critical parameter in triggering or not differentiation as their surface energies

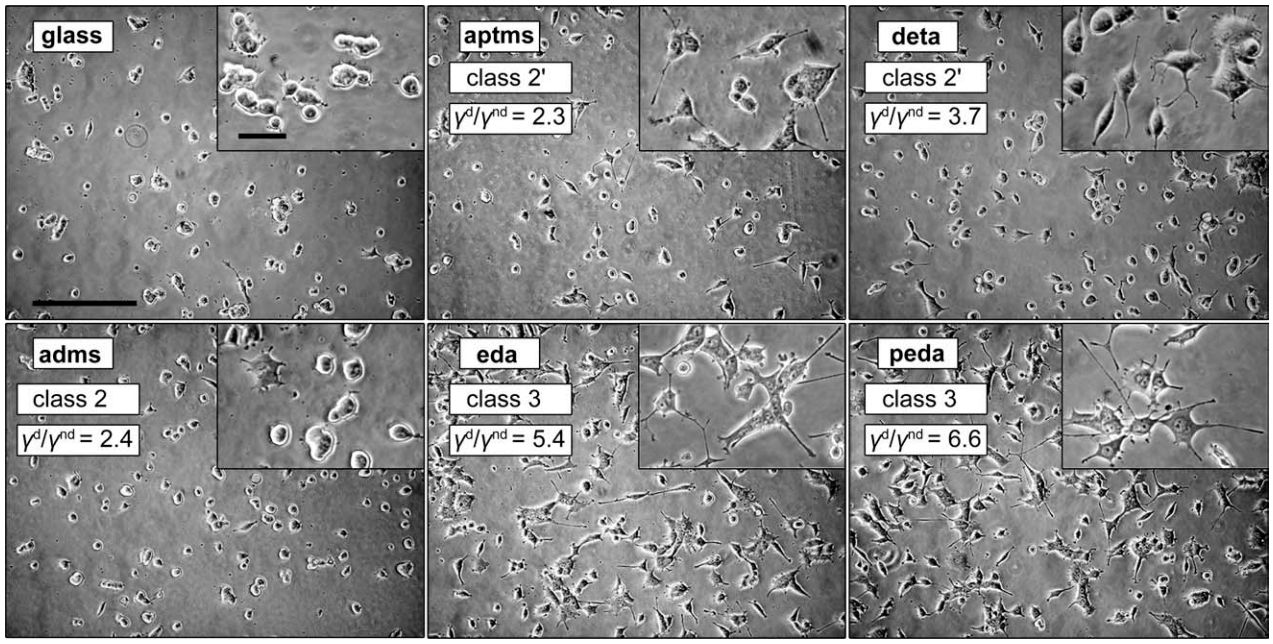

FIGURE 6. PC12 cells 24 h after seeding in NGF-free medium. γ^d and γ^{nd} are respectively the dispersive and polar components of the surface tension, displayed in Figure 5 and Table II. Cell shape appears to be controlled by distinct distributions of surface potentials, indicated by γ^d/γ^{nd} for each surfaces. PC12 cells adhered poorly on clean glass and quite fairly on class 2 (adms) and class 2′ (aptms) SAMs. Yet, their adhesion was even stronger on class 3 SAMs (eda and peda), where cells showed signs of polarization (inset boxes) and generated more neurites. On a deta substrate, cells behaved as they did on class 2 and class 2′ SAMs, indirectly indicating the surface organization of this substrate, for which surface analysis could hardly determine whether it was a class 2 or a class 3 SAM. Observations were made with an optical phase-contrast microscope. Scale bar: 250 μm (inset boxes: 50 μm), applies for all images.

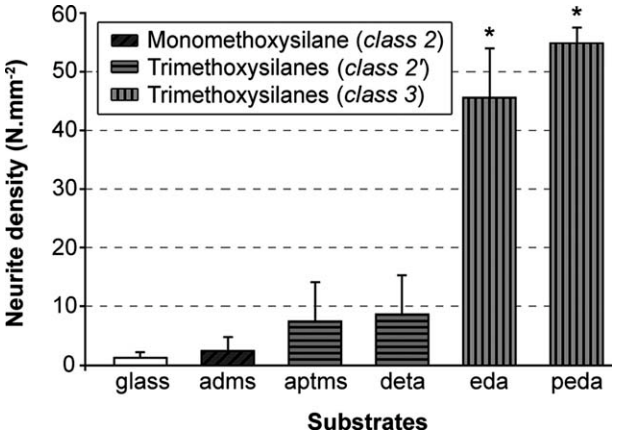

FIGURE 7. Propensity of PC12 cells to initiate neurite outgrowth without NGF treatment according to the substrate and 24 h after seeding. Pictures were taken from several fields of cells grown on each substrate, and the number of grown neurites ($L > 25$ μm) was counted. Values were compared with those of neurites extended on adms surfaces. The data reflect typical differences between substrate classes. On class 2 SAMs and class 2′ SAMs, cells adhered but initiated few neurites. On class 3 SAMs, adhesion was enhanced and cells generated more neurites [$p < 0.001$ (*)]. It is to be noticed that class 2′ SAMs seemed more favorable for neuritogenesis than a canonical class 2 SAM such as the adms substrate, though statistical differences can hardly be considered significant ($p = 0.29$ for aptms and $p = 0.20$ for deta). The density of neurites generated by PC12 cells on deta substrate suggests that it may be a class 2′ SAM, while surface analysis did not allow its classification. Bars represent SE of the mean. $N = 3$ independent measurements for each condition.

are comparable (50–55 mN m^{-1}). Although γ_s is similar for all substrates, high levels of neuritogenesis is observed when cells were seeded on class 3 surfaces, and low levels when seeded on class 2 surfaces. Class 3 surfaces exhibit a highly disordered nanoscale mixture of NH_2 and OH groups, thus generating significant local gradients in energy of adhesion, whereas class 2 SAMs are rather homogeneous. Therefore, we believe that these local gradients are the critical surface signal that triggers PC12 neuronal differentiation (see Fig. S3 in the Supporting Information), by displaying spatial variations of the surface potentials all along the cell membrane.

PC12 cells spread very well on eda and on peda substrates indicating a good adhesion to the substrate. Cells also showed signs of polarization (Fig. 6, inset boxes), what prefigures neurite extension.[32] Additionally, PC12 cells generated a comparable high density of neurites, whether seeded on eda (45 mm^{-2}) or on peda (55 mm^{-2}) (Fig. 7), both surfaces displaying similar γ_c ($\geq$42 mN m^{-1}) and distribution of surface energy components ($\gamma^d/\gamma^{nd} \geq 5.4$) characteristic of ($NH_2$/OH) class 3 SAMs. Likewise, cells produced a low number of neurites on both class 2 SAMs adms and aptms that shared similar surface energy parameters ($\gamma_c \leq 28$ mN m^{-1} and $\gamma^d/\gamma^{nd} \leq 2.4$). However, a difference in neurite density was noted between adms (3 mm^{-2}) and aptms (8 mm^{-2}) that might be related to a difference in their nanostructures. As seen above, the aptms substrate is a class 2′ SAM, which means that few parts of the aptms surface might exhibit class 3 NH_2/OH structure. This would explain that cells generated more neurites on aptms than on a canonical class 2 surface (i.e., adms) but that they spread less and developed less neurites than on class 3 substrates (i.e., eda or peda).

Neuritogenesis appears to be controlled according to the distribution of γ^d and γ^{nd}. Surfaces which distribution of SFE components verified $\gamma^d/\gamma^{nd} \leq 3.7$ poorly triggered neurite outgrowth, whereas on surfaces displaying $\gamma^d/\gamma^{nd} \geq 5.4$ many more neurites were initiated (Figs. 5 and 6). However, testing these results against those obtained with CH_3-terminated alkylsiloxanes SAMs[16] suggests that diverse distributions of long- and short-range interactions can lead similarly to PC12 differentiation, providing the surface chemical nature (CH_3/OH or NH_2/OH) is different. Actually, CH_3/OH class 3 surfaces exhibiting γ^{nd} ($\geq$20.9 mN m^{-1}) and γ^d ($\leq$27.3 mN m^{-1}) that were significantly different than the γ^{nd} ($\leq$7.8 mN m^{-1}) and the γ^d ($\geq$42.4 mN m^{-1}) of the NH_2/OH class 3 surfaces considered here, proved to be as suitable to PC12 adhesion and differentiation (cf., Ref. 16, Figs. 4 and 5). We also note that, even though high levels of neuritogenesis seem to correlate here with high γ_c values, it is likely that the absolute γ_c value is not a critical parameter in itself since in other systems,[16] surfaces sharing similar γ_c values ($19.9 < \gamma_c < 26.7$ mN m^{-1}) but significantly lower to that of eda and peda (that display $\gamma_c \geq 42$ mN m^{-1}) could trigger different cell responses, including PC12 differentiation and neuritogenesis. Therefore, we hypothesize that, rather than a particular value of γ_c, or a particular combination of γ^d and γ^{nd}, which primarily reflect macroscopic surface properties, cells respond to the way these SFE potentials are spatially distributed at the nanoscale level along the substrate surfaces. This interpretation is supported by the fact that greater chemical nano-heterogeneities seem to better stimulate the neuritogenesis (as suggested for eda and peda surfaces, which θ_{AR} values are the greatest of all the surfaces displaying very low nanoroughness).

Seeded on a clean glass surface, PC12 cells adhered poorly (Fig. 6) though clean glass surface tension ($\gamma_c \geq 150$ mN m^{-1}) is far higher than that of all other substrates ($\gamma_c \leq 44$ mN m^{-1}). We note that in ambient (P,V) conditions, clean glass is hydrated, leading to a γ_c value that should be lower than 150 mN m^{-1}, but still ranging in values ($\geq$70 mN m^{-1}) higher than all other substrates. By 24 h of seeding, some cells were observed that floated over the surface, and others had begun to aggregate to each other. During the following days of culture, the vast majority of PC12 cells appeared to be trapped into aggregates comparable in size and in shape to those we previously observed on CH_3-terminated class 2 surfaces.[16] In fact, cell clusters formation is believed to extend cell lifetime on a surface that does not favor cell adhesion. In view of these observations, we hypothesize that the adhesion of PC12 cells is intrinsically impeded on clean glass.

PC12 extension was similar whether seeded on an aptms or on a deta substrate (Figs. 6 and 7). Surface characterization exploiting the theory of Zisman was not sufficient to clearly ascribe the deta substrate either to a class 2 or to

a class 3 SAM (Fig. 3). Even if the γ_c of the deta substrate (38 mN m^{-1}), though smaller, is nevertheless close to the γ_c of class 3 surfaces ($\geq$42 mN m^{-1}), cell shape when seeded on deta is rather comparable to cell shape on a class 2′ surface like aptms. Indeed, the density of generated neurites is similar for both substrates (8 mm^{-2} for aptms and 9 mm^{-2} for deta). These data suggest that a non-negligible amount of DETA monomers are rather in an ordered organization than in a disordered one. As a result, the deta surface might be considered as a class 2′ SAM. It is to be noted that here, cells can be used as "probes" to detect a surface nanostructure.

In summary, surface analyzes indicate that deta nanostructure is rather a class 3 SAM than a class 2 SAM, whereas cell observation suggests the opposite. To explain this, we hypothesize that the deta substrate does exhibit local gradients in surface energy, but not as high as those displayed by the eda and peda surfaces. That cells detect a gradient over a threshold value remains to be determined (for instance, using patterned surfaces with controlled gradients at the nanometer scale), since the gradients can theoretically emerge out from the surface as soon as a few OH groups appear in a NH_2-continuum.

How do cells respond to nanoscale surface characteristics?

Beyond explaining how cells "sense" the surface energy gradients, the modeling of neurite formation process[33] suggests how cells could be affected by nanoscale chemical heterogeneities. Some authors have suggested that the initiation of a neurite could be the result of spontaneous membrane oscillations.[34,35] In this model, local membrane heterogeneities produce focal depolarization that lead to an increase of calcium and sodium ions entry inside the cell.[36] The translocation of these ions would then induce a positive feedback, driving more ions to pass through the cell membrane and eventually lead to the initiation of a neurite. Within the framework of this model, it appears possible that local gradients in interactions (distribution of long-, short-range interactions) in substrate surfaces would stimulate local membrane oscillations (attraction/repulsion), which would in turn induce neuritogenesis by activating the positive feedback of calcium and sodium ion entry.

This hypothesis is sustained by observations made by reflexion interference contrast microscopy,[15] in which we found that seeded on a homogeneous amine-terminated substrate, the vast majority of PC12 cell surface was in close contact with the substrate. Conversely, on a heterogeneous NH_2/OH substrate, cell–substrate close–contact areas were in low proportions, suggesting that the amplitude of membrane oscillations was increased, eventually driving PC12 cells to generate neurites. In addition, it was shown that calcium transients through filopodia could promote substrate-dependent growth cone turning.[37] It is thus likely that substrate-induced PC12 differentiation relies on a mechanism that would involve the cooperation of filopodial and/or lamellipodial membrane movements with external factors, such as calcium transients.

CONCLUSIONS

PC12 cell ability to undergo neuritogenesis was assessed according to surface ordering, and thus to surface free-energy distribution. Our results indicate that PC12 cells were sensitive to the nanoscale spatial distribution of surface potentials, rather than to the total surface tension. A range of NH_2-terminated self-assembled monolayers with varying surface energy distributions were successfully prepared. We characterized their chemical structure as predominated by a rather homogeneous (i.e., class 2) or heterogeneous (i.e., class 3) nanoscale organization. Seeded on class 3 surfaces, PC12 cells adhered well and full neuritogenesis was obtained by less than 24 h of culture without NGF treatment. Data presented here combined to previous observations provide an overall outlook on PC12 cells interaction with stiff model surfaces: on homogeneous surfaces (composed of either CH_3, NH_2, or OH groups), PC12 cell adhesion is modulated by the chemical affinity to each of these groups, and even when adhesion is favored, that is, on NH_2-surfaces, only few neurites are generated. Conversely, on highly heterogeneous substrates (composed of a nanoscale mixture of either CH_3/OH or NH_2/OH groups, whether or not intrinsically favorable to the cells), adhesion is greatly enhanced and high levels of neuritogenesis are observed. Future work should determine whether other cell types such as myoblasts or osteoblasts are also sensitive to the nanoscale distribution of surface potentials.

ACKNOWLEDGMENTS

The authors thank Dr. Michel Nardin for thoughtful comments that seeded the initial idea of this work.

REFERENCES

1. Franze K, Guck J. The biophysics of neuronal growth. Rep Prog Phys 2010;73:094601.1–094601.19.
2. Hoffman-Kim D, Mitchel JA, Bellamkonda RV. Topography, cell response, and nerve regeneration. Annu Rev Biomed Eng 2010; 12:203–231.
3. Roach P, Parker T, Gadegaard N, Alexander MR. Surface strategies for control of neuronal cell adhesion: A review. Surf Sci Rep 2010;65:145–173.
4. Schwarz US, Bischofs IB. Physical determinants of cell organization in soft media. Med Eng Phys 2005;27:763–772.
5. Liu XA, Chen J, Gilmore KJ, Higgins MJ, Liu Y, Wallace GG. Guidance of neurite outgrowth on aligned electrospun polypyrrole/poly(styrene-beta-isobutylene-beta-styrene) fiber platforms. J Biomed Mater Res Part A 2010;94:1004–1011.
6. Staii C, Viesselmann C, Ballweg J, Shi L, Liu G-y, Williams JC, Dent EW, Coppersmith SN, Eriksson MA. Positioning and guidance of neurons on gold surfaces by directed assembly of proteins using atomic force microscopy. Biomaterials 2009;30:3397–3404.
7. Xiong Y, Lee AC, Suter DM, Lee GU. Topography and nanomechanics of live neuronal growth cones analyzed by atomic force microscopy. Biophys J 2009;96:5060–5072.
8. Lee MH, Brass DA, Morris R, Composto RJ, Ducheyne P. The effect of non-specific interactions on cellular adhesion using model surfaces. Biomaterials 2005;26:1721–1730.
9. Lee SJ, Khang G, Lee YM, Lee HB. The effect of surface wettability on induction and growth of neurites from the PC-12 cell on a polymer surface. J Colloid Interface Sci 2003;259:228–235.
10. Stenger DA, Pike CJ, Hickman JJ, Cotman CW. Surface determinants of neuronal survival and growth on self-assembled monolayers in culture. Brain Res 1993;630:136–147.
11. Engler AJ, Sen S, Sweeney HL, Discher DE. Matrix elasticity directs stem cell lineage specification. Cell 2006;126:677–689.

12. Franze K, Gerdelmann J, Weick M, Betz T, Pawlizak S, Lakadamyali M, Bayer J, Rillich K, Gögler M, Lu YB, Reichenbach A, Janmey P, Käs J. Neurite branch retraction is caused by a threshold-dependent mechanical impact. Biophys J 2009;97:1883–1890.
13. Gunn JW, Turner SD, Mann BK. Adhesive and mechanical properties of hydrogels influence neurite extension. J Biomed Mater Res Part A 2005;72:91–97.
14. Murnane AC, Brown K, Keith CH. Preferential initiation of PC12 neurites in directions of changing substrate adhesivity. J Neurosci Res 2002;67:321–328.
15. Lamour G, Journiac N, Souès S, Bonneau S, Nassoy P, Hamraoui A. Influence of surface energy distribution on neuritogenesis. Colloids Surf B 2009;72:208–218.
16. Lamour G, Eftekhari-Bafrooei A, Borguet E, Souès S, Hamraoui A. Neuronal adhesion and differentiation driven by nanoscale surface free-energy gradients. Biomaterials 2010;31:3762–3771.
17. Mischel PS, Umbach JA, Eskandari S, Smith SG, Gundersen CB, Zampighi GA. Nerve growth factor signals via preexisting TrkA receptor oligomers. Biophys J 2002;83:968–976.
18. Wehrman T, He X, Raab B, Dukipatti A, Blau H, Garcia KC. Structural and mechanistic insights into nerve growth factor interactions with the TrkA and p75 receptors. Neuron 2007;53:25–38.
19. Greene LA, Tischler AS. Establishment of a noradrenergic clonal line of rat adrenal pheochromocytoma cells which respond to nerve growth factor. Proc Natl Acad Sci USA 1976;73:2424–2428.
20. Cooke MJ, Zahir T, Phillips SR, Shah DSH, Athey D, Lakey JH, Shoichet MS, Przyborski SA. Neural differentiation regulated by biomimetic surfaces presenting motifs of extracellular matrix proteins. J Biomed Mater Res Part A 2010;93:824–832.
21. Fujii DK, Massoglia SL, Savion N, Gospodarowicz D. Neurite outgrowth and protein synthesis by PC12 cells as a function of substratum and nerve growth factor. J Neurosci 1982;2:1157–1175.
22. Wujek JR, Akeson RA. Extracellular matrix derived from astrocytes stimulates neuritic outgrowth from PC12 cells in vitro. Brain Res 1987;431:87–97.
23. Zisman WA. Contact angle, wettability and adhesion. Adv Chem Ser 1964;43:1–51.
24. Owens DK, Wendt RC. Estimation of surface free energy of polymers. J Appl Polym Sci 1969;13:1741–1747.
25. Impens N, van der Voort P, Vansant EF. Silylation of micro-, meso- and non-porous oxides: A review. Microporous Mesoporous Mater 1999;28:217–232.
26. Kanan SA, Tze WTY, Tripp CP. Method to double the surface concentration and control the orientation of adsorbed (3-aminopropyl)dimethylethoxysilane on silica powders and glass slides. Langmuir 2002;18:6623–6627.
27. Lamour G, Hamraoui A, Buvailo A, Xing Y, Keulayan S, Prakash V, Eftekhari-Bafrooei A, Borguet E. Contact angle measurements using a simplified experimental setup. J Chem Edu 2010;87:1403–1407.
28. Fisher JC. The fracture of liquids. J Appl Phys 1948;19:1062–1067.
29. de Gennes PG, Brochard-Wyart F, Quéré D. Capillarity and Wetting Phenomena: Drops, Bubbles, Pearls, Waves. New York: Springer-Verlag; 2003. 291 p.
30. de Gennes PG. Wetting—Statics and dynamics. Rev Mod Phys 1985;57:827–863.
31. Wirth MJ, Fatunmbi HO. Horizontal polymerization of mixed trifunctional silanes on silica—A potential chromatographic stationary phase. Anal Chem 1992;64:2783–2786.
32. Matta LL, Aranda-Espinoza H. Neuronal systems and modeling: Strong adhesion identifies potential neurite extension and polarization sites in PC12 cells. Biophys J 2008;94:1055–1057.
33. Graham BP, van Ooyen A. Mathematical modelling and numerical simulation of the morphological development of neurons. BMC Neurosci 2006;7:S9.1–S9.12.
34. Hentschel HGE, Fine A. Instabilities in cellular dendritic morphogenesis. Phys Rev Lett 1994;73:3592–3595.
35. Hentschel HGE, Fine A. Early dendritic and axonal morphogenesis. In: van Ooyen A, editor. Modeling Neural Development. Cambridge MA: MIT Press; 2003. p 49–74.
36. Veksler A, Gov NS. Calcium-actin waves and oscillations of cellular membranes. Biophys J 2009;97:1558–1568.
37. Gomez TM, Robles E, Poo M, Spitzer NC. Filopodial calcium transients promote substrate-dependent growth cone turning. Science 2001;291:1983–1987.